Journal of Sustainable Development of Energy, Water and Environment Systems

http://www.sdewes.org/jsdewes

Year 2026, Volume 14, Issue 2, 1140699

Original Research Article

Renewable Energy Resources Optimization for Green Hydrogen Production at Lüderitz, Namibia

Ernesto T.O Samuel[*1], Tom Wanjekeche[1], Andreas Ndapuka[1], Kai Holtappels[2], Josua Junias[1,2]*

[1]Department of Electrical and Computer Engineering, University of Namibia, Ongwediva, Namibia
[2]Division of safety of Energy Carriers, Bundesanstalt für Materialforschung und -prüfung (BAM), Berlin, Germany
e-mail: 201707633@students.unam.na, twanjekeche@unam.na, andapuka@unam.na, kai.holtappels@bam.de, josua-kondja.junias@bam.de

Cite as: Samuel, E., Wanjekeche, T., Ndapuka, A., Holtappels2, K., Junias, J., Renewable Energy Resources Optimization for Green Hydrogen Production at Lüderitz, Namibia, J.sustain. dev. energy water environ. syst., 14(2), 1140699, 2026, DOI: https://doi.org/10.13044/j.sdewes.d14.0699

ABSTRACT

Green hydrogen is poised to be a critical vector in the global energy transition and plays a crucial role in reducing carbon emissions and creating a global clean energy market. However, the economic viability of large-scale green hydrogen production hinges on the optimal design and location. Namibia has an excellent wind and solar energy potential, enabling a feasible, cost-effective green hydrogen production from intermittent renewable energy. This study developed a techno-economic optimization model for cost-effective green hydrogen facilities in Namibia using a single-objective genetic algorithm to determine the optimal wind, solar, and battery storage capacities needed to meet an annual production target of 355,000 tons at Luderitz, Namibia. The model runs on an hourly time-series simulation and uses a discounted cash flow method to minimize the levelized cost of hydrogen for a full year. The results of the optimized system gave a levelized cost of hydrogen of 2.50 USD/kg compared to 7.5 USD/kg obtained from a study on local hydrogen production analysis. This demonstrated the superior performance of the proposed algorithm. A sensitivity analysis was performed on the green hydrogen system, using different numbers of electrolyzers. A range of 150 to 200 units each rated 17.5 MW. Using the proposed algorithm, it was discovered optimal number of Electrolyzers that results in optimal cost of hydrogen is between 196 and 200 units. The findings demonstrated that the levelized cost of hydrogen is not just an average value, as had been demonstrated by various documented publications.

KEYWORDS

Electrolyser, Genetic algorithm, Green hydrogen, Levelized cost of hydrogen, Net present value, Optimization, Renewable energy sources.

INTRODUCTION

Energy consumption, greenhouse gas emissions, and air pollution continue to rapidly increase, therefore prompting a need to develop and introduce new alternatives to fossil fuels [1]. Green hydrogen is a promising solution towards the decarbonization of global energy systems, as it can be used for long-term energy storage from renewable energy sources, for the substitution of fossil fuels in transport and heating sectors, and as a clean feedstock for processing industries [1]. However, all green hydrogen production methods are still under research [2]; hence, no feasible cost-effective commercial green hydrogen production method

[*] Corresponding author

is available to date. Renewable power generation costs have fallen sharply over the past decade, driven by steadily improving technologies, economies of scale, competitive supply chains, and improving developer experience [3]. This decrease in the cost of renewable energy products will result in a decrease of overall costs of hydrogen systems.

Both wind and solar generation produce electricity intermittently, depending on wind speed and solar radiation. Consequently, spatio-temporal variability in climatic and seasonal conditions results in distinct generation profiles, characterized by significant geographical and fluctuations in power output [4]. It is crucial to study the complementary status of different renewable energy sources (RESs) by analyzing their combined capacity factor in different seasons. Namibia's solar and wind energy capabilities, their complementary status, and propinquity to seawater on the coast, can generate green hydrogen at a global scale. This will involve using its abundant solar and wind resources to drive seawater desalination plants to provide water which can be split into hydrogen and oxygen using electrolyzers driven by electricity generated by renewable sources.

Although electrochemical storage systems like lithium-ion batteries are used, their high capital expenditure and limited long-duration capacity present significant economic barriers to the deployment of utility-scale RES installations [5], [6]. Hydrogen storage in the form of ammonia and its conversion to electricity using fuel cells has demonstrated potential in balancing supply and demand in renewable energy grids, potentially reducing fluctuations of intermittent RESs [7]. Hence, hydrogen produced from renewable energy resources will meet or exceed storage energy requirements in renewable energy systems[6]. The defining characteristic of green hydrogen is its zero-carbon production process, positioning it as a critical asset for decarbonizing the energy, transportation, and industrial sectors as part of the global energy transition. At this stage, green hydrogen accounts for only a small percentage of total hydrogen production due to the high costs associated with its production process. However, it has an excellent projection towards the future, being the cleanest hydrogen type, which will help to satisfy net-zero carbon plans [8].

Recent research has increasingly focused on optimizing renewable-powered hydrogen systems using techno-economic and optimization frameworks. Several studies have investigated hybrid renewable systems that integrate solar PV, wind power, and hydrogen production. For example, Akarsu and Serdar [9] investigated the design of a microgrid system consisting of hybrid renewable energy integration to meet a residential annual load in Kayseri region. The results demonstrated that by combining solar, wind, diesel generator, battery, and hydrogen storage, their optimized hybrid system is economically viable, and the cost of energy is 0.376 USD/kW. Mohammad and Iqbal in [10] analysed a solar-powered energy system designed for green hydrogen generation, using optimization techniques and dynamic simulations to assess system performance. Their results showed a cost-effective system configuration that could produce hydrogen at 4.806 USD/kg, with a total lifetime expenditure of USD 749,904. Their study confirmed that photovoltaic-based hydrogen production is both technically viable and economically competitive. Similarly, Barhoumi *et al.* [11] optimized the production of hydrogen from hydroelectric-photovoltaic and the power grid. Their overall analysis found that the net profit plays a crucial role in optimizing the levelized cost of green hydrogen, which was determined to be 2.25 EUR/kg. Alhussan *et al*. [12] used Al-Biruni Earth Radius (BER) and Particle Swarm Optimization (PSO) to ensemble forecast solar hydrogen generation. Their method optimizes the dynamic parameters of the deep learning model of recurrent neural network (RNN) using the BER metaheuristic search optimization algorithm and the PSO algorithm. Their results show that the solar system could produce, on average, 0.622 kg/day of hydrogen during the season. Park *et al.* [13] presented a multi-objective optimization-based framework for solar-powered green hydrogen for optimal system design that balances economic cost and productivity. Their system uses meteorological data to estimate how much solar power would be generated and how much hydrogen would be produced as a result. The optimization framework is suggested for calculating and simultaneously optimizing the amount of hydrogen produced and the levelized cost of hydrogen (LCOH). Their results show that an optimal system size exists for each different objective, and that a significant improvement in LCOH can be accomplished by enhancing the components' cost and performance. It is further revealed that the optimal electrolyser size to minimize LCOH is roughly 60% of the solar power capacity, and installing batteries is ineffective for boosting economic viability, but can improve hydrogen production by utilizing unused electricity during the peak period.

However, despite the growing interest in green hydrogen systems, several research gaps remain. First, the majority of existing studies still concentrate on small-scale hydrogen production, limiting the transferability of insights to utility-scale projects. Second, only a limited number of investigations evaluate full-year (8,760 hour) operational dynamics, which are essential for capturing seasonal variability and the complementary nature of solar and wind resources. In addition, many studies overlook detailed operational constraints of key system components, including electrolyzer minimum load limits, wind turbine cut-in and cut-out speeds, and battery state-of-charge boundaries. Finally, there is very limited literature that specifically examines the green hydrogen production potential of Lüderitz, Namibia, despite its globally competitive renewable resource profile.

This research focuses on the critical interplay between intermittent RESs: wind and solar, and the high capital cost of battery storage. The main objective of this study is to perform technical and economic analysis of green hydrogen production at Lüderitz, Namibia, by (a) developing a techno-economic model of Wind-Photovoltaic-Battery-Desalination-Electrolysis (WPBDE) system and (b) optimizing the model for improved system performance that results in optimal levelized cost of electricity, and LCOH. The LCOH represents the average break-even price per kilogram of hydrogen produced over the project's entire lifetime. Therefore, optimizing the configuration and operation of these interconnected technologies is paramount to ensuring a stable power supply for electrolyzers and accelerating the transition to a sustainable hydrogen economy.

The optimization process is performed using a single-objective Genetic Algorithm (GA), a robust heuristic search method well-suited for complex, non-linear problems with integer variables [14]. The GA optimization was selected for this application due to the specific nature of our problem, which is characterized as a Mixed-Integer Non-Linear Programming (MINLP) problem. Other optimization approaches, such as gradient-based methods, were not considered as they require a smooth, differentiable objective function to determine gradients. This determines optimal values for the objective function (LCOH), which is an output of a complex variable developed over an 8760-hour simulation period. The process is discrete in nature, such as electrolyzers' switching on/off, which results in a non-differentiable and hence, using gradient-based methods is not possible. Linear Programming (LP) and its variants are highly efficient but are limited to solving problems where both objective function and all constraints are linear. The relationship between renewable power generation, battery dispatch, and hydrogen production in this study's model is non-linear, immediately disqualifying LP as a viable approach.

MATERIALS AND METHODS

This section details the analytical framework and technical approach used to evaluate the feasibility and efficiency of an optimized green hydrogen production system.

Proposed System Configuration

The proposed system configuration for green hydrogen production consists of 5 subsystems: wind turbines, solar PV arrays, a Battery Energy Storage System (BESS), a Proton Exchange Membrane (PEM) electrolyzer plant and a Reverse Osmosis (RO) desalination plant as shown in Figure 1.

BESS is incorporated to buffer fluctuations in generation and improve the utilization rate of the electrolyzer by smoothing short to medium-term intermittencies. The PEM electrolyzer receives input power from either combined RESs or from both the battery and RESs, depending on power availability and sub-systems state. A supervisory control layer dynamically manages power dispatch among components to ensure optimal operation. As illustrated in **Figure 1**, energy flows from RESs to the electrolyzer through optimal battery buffering. The system architecture is embedded within an optimization framework that optimizes capacities of wind, solar, battery, and electrolyzer units to minimize LCOH while meeting the annual hydrogen production target of 355,000 tons. The model accounts for system constraints, efficiency losses, and hourly resolution to ensure realistic and technically viable results.

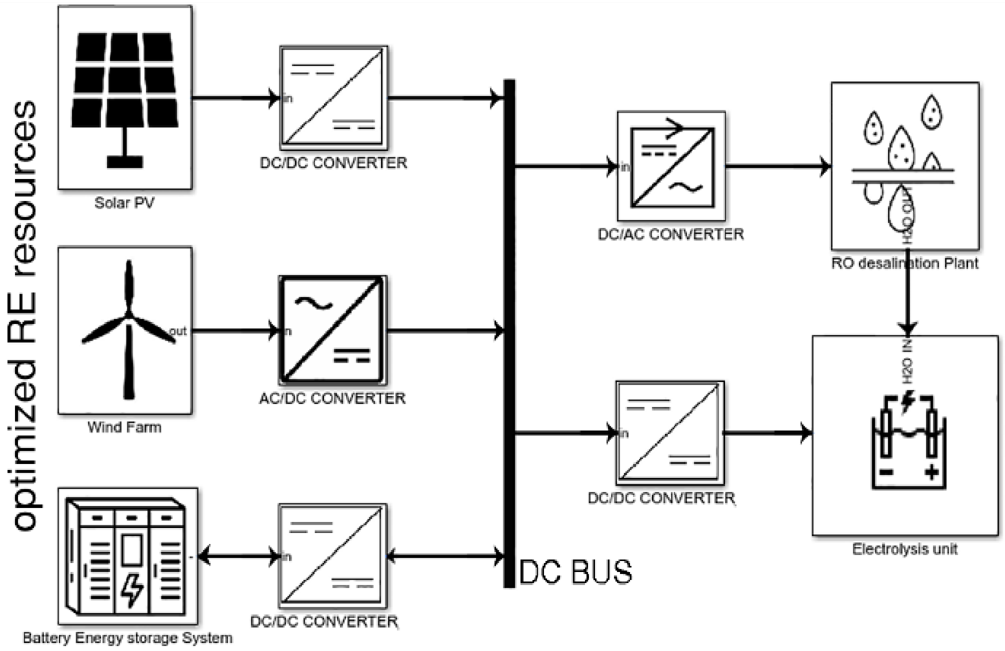

Figure 1. System configuration/model

Mathematical Modelling of System Components

This section presents the mathematical models used to describe the performance of the solar PV array, wind turbine, battery storage, and PEM electrolyzer that make up the hybrid system.

Solar PV model. A solar module is an assembly of solar cells, which are further interconnected to create solar arrays. The operating principle of solar cells is based on the photovoltaic (PV) effect, which involves the generation of a potential difference at the P-N junction when exposed to sunlight [15]. The practical characteristic of a solar cell is defined by eq. (1) [15]:

$$I = I_{\mathrm{ph}} - I_{\mathrm{d}} - I_{\mathrm{sh}} = I_{\mathrm{sh}} - I_{\mathrm{o}}\left(\mathrm{e}^{\frac{qV}{kT}} - 1\right) - I_{\mathrm{sh}} \tag{1}$$

where are: I - the output current of the PV cell (A); I_{ph} - the photocurrent (A); I_{d} - diode current (A); I_{sh} is the current lost to shunt resistance (A); I_{o} - diode saturation current (A); q - electron charge (1.602×10^{-19} C); V - the terminal voltage; k - the Boltzmann constant (1.381×10^{-23} J/K), and T - absolute temperature of the cell (K).

The generated current I_{ph}, as indicated in the literature [15], [16], [17], is defined by:

$$I_{\mathrm{ph}} = \left[I_{\mathrm{sc}} + K_{\mathrm{i}}(T_{\mathrm{r}} - T_{\mathrm{o}}) \times \left(\frac{G}{1000}\right)\right] \tag{2}$$

where are: I_{sc} - short-circuit current (A); K_i - the cell's short-circuit current temperature coefficient (A/K); T_o is the cell operating temperature (K); T_r - the cell's reference temperature (K), and G is the solar irradiance (W/m^2).

The reverse saturation current at the reference temperature is defined by **[16]** as:

$$I_{\mathrm{rs}} = \frac{I_{sc}}{\exp^{\left(\frac{qVoc}{N_s aKT_{\mathrm{O}}}\right)} - 1} \tag{3}$$

where are: I_{rs} - reverse saturation current of the diode; q - electron charge (1.602×10^{-19} C); V_{oc} is open circuit voltage (V); N_p is the cell's interconnected in parallel; N_s - cells interconnected in series; a - the ideality factor, and K - the Boltzmann constant (1.38×10^{23} J/K).

The solar cell saturation current I_0 varies with cell temperature, and is defined by **[16]** as:

$$I_{\mathrm{o}} = I_{\mathrm{rs}} \left[\frac{T}{T_{\mathrm{r}}}\right]^3 \exp\left[\frac{qE_{\mathrm{q0}}}{ak}\left(\frac{1}{T} - \frac{1}{T_{\mathrm{r}}}\right)\right] \tag{4}$$

where are: I_{rs} - reverse saturation current at reference temperature T_r; $\left(\frac{T}{T_{\mathrm{r}}}\right)^3$ - the temperature correction factor, and E_{q0} - the semiconductor band-gap energy.

Shunt current is defined in **[15]**, **[16]**, **[17]** as:

$$I_{\mathrm{sh}} = \frac{V + R_{\mathrm{s}} I}{R_{\mathrm{sh}}} \tag{5}$$

where are: V - the terminal voltage of the PV cell; R_{s} - series resistance; I - output current of the PV cell, and R_{sh} - shunt resistance.

Therefore, the current of a solar PV is defined by **[15]** as:

$$I_{\mathrm{pv}} = N_{\mathrm{p}} \times I_{\mathrm{ph}} - N_{\mathrm{p}} \times I_{\mathrm{o}} \left[\left(\exp^{\frac{qVpv}{N_s AKT}} - 1\right)\right] - I_{\mathrm{sh}} \tag{6}$$

The efficiency η of a solar module is the ratio of output power to input power and is defined by:

$$\eta = \frac{P_{\mathrm{max}}}{P_{\mathrm{in}}} \tag{7}$$

where are: P_{max} - *the* maximum output power and P_{in} is the input power.

Wind power. Wind to power involves wind turbines that convert wind's kinetic energy with their rotating blades to spin a generator. The generator then converts this mechanical energy into electrical energy via electromagnetic induction, producing an electric current. The mathematical model equations for wind to power are defined by eq. (8) to eq. (13) [18]:

Kinetic power of wind passing through a turbine's swept area is defined by:

$$P_{\mathrm{k}} = \frac{1}{2}\rho A v^3 \tag{8}$$

where are: ρ - air density (m^3/kg); v - wind speed (m/s), and A - the swept area of the turbine blades.

The swept area of the turbine blades is defined by:

$$A = \pi R^2 \tag{9}$$

where R (m) is the blade radius.

Mechanical power extracted from the wind turbine is defined by:

$$P_{\mathrm{mech}} = C_{\mathrm{p}}\ (\lambda, \beta)\ P_{\mathrm{k}} \tag{10}$$

where are: P_{mech} - mechanical power (kW); C_{p} - the power coefficient ($0 < C_{\mathrm{p}} < 0.59$); β - the blade pitch angle (°), and λ - the tip speed ratio (-).

Tip speed ratio is defined by:

$$\lambda = \frac{\omega R}{v} \tag{11}$$

where are: ω - the rotational speed (rad/s) and R - the blade radius (m).

After mechanical losses and generator efficiency, the equivalent electrical power is defined by:

$$P_{\mathrm{elec}} = \eta_{\mathrm{gen}} \times \eta_{\mathrm{gear}} \times P_{\mathrm{mech}} \tag{12}$$

where are: P_{elec} - the equivalent electrical power (kW); η_{gen} - the generator efficiency (%), and η_{gear} - the gearbox efficiency (%).

The turbine's power output depends on wind speed (v):

$$P_{\mathrm{elec}}(v) = \begin{cases} 0 & v < v_{\mathrm{cut-in}} \\ k \times v^3 & v_{\mathrm{cut-in}} \leq v < v_{\mathrm{rated}} \\ P_{\mathrm{rated}} & v_{rated} \leq v < v_{\mathrm{cut-out}} \\ 0 & v \geq V_{\mathrm{cut-out}} \end{cases} \tag{13}$$

where are: $v_{\mathrm{cut-in}}$ speed is the minimum speed (m/s), v_{rated} - maximum power speed (m/s); $v_{\mathrm{cut-out}}$ is cut-out speed (m/s); k - a turbine constant (-), and P_{rated} - the maximum rated power.

<u>*Battery energy storage system (BESS)*</u>. The battery energy storage (Li-ion) is modelled in terms of charge and discharge characteristics. The circuit equivalent diagram of the Lithium-ion battery is shown in Figure 2 below [19].

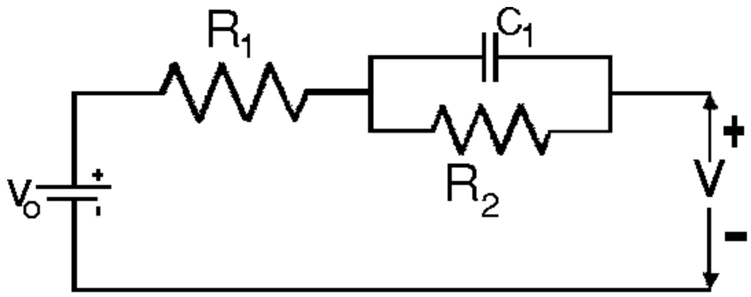

Figure 2. Electrical equivalent circuit of a Li-ion battery

From **Figure 2**, V_o is the open circuit voltage, R_1 and R_2 represent internal resistance, and C_1 is the effective capacitance of the battery. State of Charge (*SOC*) of a lithium-ion battery is a key parameter indicating the remaining available energy as a percentage of its fully charged capacity. Coulomb's current integration mathematical model for SOC estimation is presented by eq. (14) and eq. (15) below **[20]**:

$$SOC(t) = SOC_0 - \frac{1}{Q_\mathrm{n}} \int_0^t \eta \times I(t)\mathrm{d}t \tag{14}$$

where are: *SOC* (*t*) - the State of Charge at time *t*; SOC_0 - the initial *SOC*; Q_n - the nominal battery capacity (Ah); *I*(*t*) - the battery current (positive during discharge, negative during charge), and η - Coulombic efficiency.

To protect battery life, limits are applied:

$$SOC_\mathrm{min} \leq SOC(t) \leq SOC_\mathrm{max} \tag{15}$$

where are: SOC_min - the minimum *SOC* and SOC_max is the maximum *SOC*.

<u>*PEM electrolyser*</u>. Modelling of the PEM electrolyser to determine its efficiency under varying weather conditions and capacity in terms in terms of hydrogen production is as given by equations (16)-(27) **[21]**.

Electrolyzer electrical power is expressed by as:

$$P_\mathrm{ele} = \frac{V_\mathrm{cell}^2}{R_\mathrm{T}} \tag{16}$$

where are: V_cell - the cell voltage and R_T is the total resistance.

The total resistance, R_T, is also defined as:

$$\frac{1}{R_\mathrm{T}} = \frac{1}{R_\mathrm{ele}} + \frac{1}{R'} \tag{17}$$

Molar energy stored across the electrical load enables the process of water electrolysis and is calculated by:

$$G_\mathrm{E} = \frac{P_\mathrm{E}}{\dot{n}} \tag{18}$$

where are: G_{E} is molar electrical energy; P_{E} - electrical power supplied to the electrolyzer (W), and $\dot{n}$ - molar flow rate of hydrogen (mol/s).

Electrolysis will only take place the minimum amount of energy required is as given by eq. (19):

$$G_{\min} = \Delta H - \frac{T}{T_0} T_{\Delta \mathrm{S}} \tag{19}$$

where are: ΔH - water enthalpy; $T_{\Delta\mathrm{S}}$ is reaction entropy; T - water temperature, and T_0 - the reference temperature.

For further analysis of the system, mole rate of both the electrons ($\mathrm{mol_e}$) hydrogen $\mathrm{mol_{H2}}$ in the electrolyzer, are determined by eq. (20) and eq. (21):

$$\mathrm{mol_e} = \begin{cases} \dfrac{\mu(G_{\mathrm{E}} - G_{\min})}{e_{\mathrm{v}} N_{\mathrm{A}}} & G_{\mathrm{E}} > G_{\min} \\ 0 & G_{\mathrm{E}} \leq G_{\min} \end{cases} \tag{20}$$

$$\mathrm{mol_{H2}} = \begin{cases} \dfrac{N_{\mathrm{c}} \mathrm{mol_e}}{2} & G_{\mathrm{E}} > G_{\min} \\ 0 & G_{\mathrm{E}} \leq G_{\min} \end{cases} \tag{21}$$

where are: N_{A} - Avogadro constant; e_{V} - energy per electron; N_{c} - the number of cells; μ - the temperature-dependent efficiency of the electrolysis.

The current flowing through the electrolyzer tank is defined by:

$$I = \mathrm{mol_e} F \tag{22}$$

where F is the Faraday constant.

The mass rates of consumed water and generated hydrogen can be calculated by using eq. (23) and eq. (24):

$$\dot{m}_{\mathrm{H2O}} = \dot{\mathrm{m}}\mathrm{ol_{H2}} M_{\mathrm{H20}} \tag{23}$$

$$\dot{m}_{H2} = \dot{\mathrm{m}}\mathrm{ol_{H2}} M_{\mathrm{H2}} \tag{24}$$

where are: M_{H2O} - the molar mass of water and M_{H2} - the molar mass of hydrogen.

To compute the pH of water in a tank, the electrolyser uses the following equation:

$$\mathrm{pH} = \ln\left(\frac{X_{\mathrm{hp}}}{\mathrm{mol_{H2\_acc}}}\right) \tag{25}$$

where X_{hp} is captures the floating hydrons (H+) in a solution and is defined by:

$$X_{\mathrm{hp}} = \begin{cases} \int \mathrm{mol_e} & \text{pH assumed constant} \\ \int (1 - \mathrm{purge})\mathrm{mol_e} & \text{pH assumed dynamic} \end{cases} \tag{26}$$

$\mathrm{mol_{H2\_acc}}$ is the number of moles of water defined by:

$$\mathrm{mol_{H2\_acc}} = \frac{\rho_{\mathrm{H2O}}(T)V}{M_{\mathrm{H2O}}} \tag{27}$$

where are: V - volume; $\rho_{\mathrm{H2O}}(T)$ - the density of water at temperature T, and M_{H2O} - molar mass of water (18.015 g/mol).

MATLAB Optimization Toolbox

The optimization problem formulated in this study is solved using the Global Optimization Toolbox in MATLAB. The computational experiments were performed on a workstation equipped with an 11th Gen Intel(R) Core(TM) i5-1135G7 @ 2.40 GHz (2.42 GHz) and 16 GB of RAM. To mitigate the computational burden of evaluating hourly dispatch for a population of 200 individuals, parallelization was implemented using the MATLAB Parallel Computing Toolbox. Given the presence of non-linear constraints and the potential for a non-convex search space, a Genetic Algorithm (GA) is selected as the primary solver. The GA is particularly suited for this application due to its ability to navigate complex landscapes without requiring gradient information.

To ensure the reproducibility of the results, the operational parameters are kept consistent throughout all trials. The algorithm is configured with a population size of 200 and a maximum limit of 150 generations. The specific operational parameters and genetic operators are summarized in **Table 1**. The Augmented Lagrangian method is specifically employed to manage the non-linear constraints, ensuring that the search remains within the feasible region. Furthermore, the Adaptive Feasible mutation function was selected to maintain genetic diversity while strictly respecting the defined problem boundaries. This configuration ensures that the obtained optimum is not only mathematically sound but also physically realizable within the constraints of the system.

Table 1. Operational parameters for Genetic Algorithm implementation

Parameter	**Value/setting**
Solver	Augmented Lagrangian Genetic Algorithm
Population size	200
Maximum generations	150
Selection function	Stochastic Uniform
Crossover function	Scattered (Fraction: 0.8)
Mutation Function	Adaptive Feasible
Elitism	10 individuals (5% of the population)
Constrain Handling	Augmented Lagrangian Method
Convergence Criteria	Max Stall Generations:50; Function Tolerance:10^{-6}

Optimization Implementation

Wind and solar energy sources have different availability patterns with respect to time; without proper optimization, the system may either underperform or become economically unviable. Optimization algorithms ensure the best possible configuration of wind turbines and solar panels to maximize total energy harvested from available intermittent energy resources. This includes determining optimal sizing and layout of these subsystems. By balancing the variability of wind and solar energy generation, the optimization process can ensure a more stable and predictable energy supply, reducing the need for backup power or storage. Moreover, proper energy sub-systems configuration optimization avoids over-sizing and under-utilization of components, reducing capital and operational expenditures. It ensures that investments are made efficiently.

The proposed GA iteratively refines a population of potential system designs over multiple generations to converge on a solution that minimizes the objective function while adhering to all specified constraints.

The flowchart shown in **Figure 3** provides a visual representation of the iterative process undertaken by the GA used in this study, from the initialization of a random population of system designs to the final selection of the single optimal configuration.

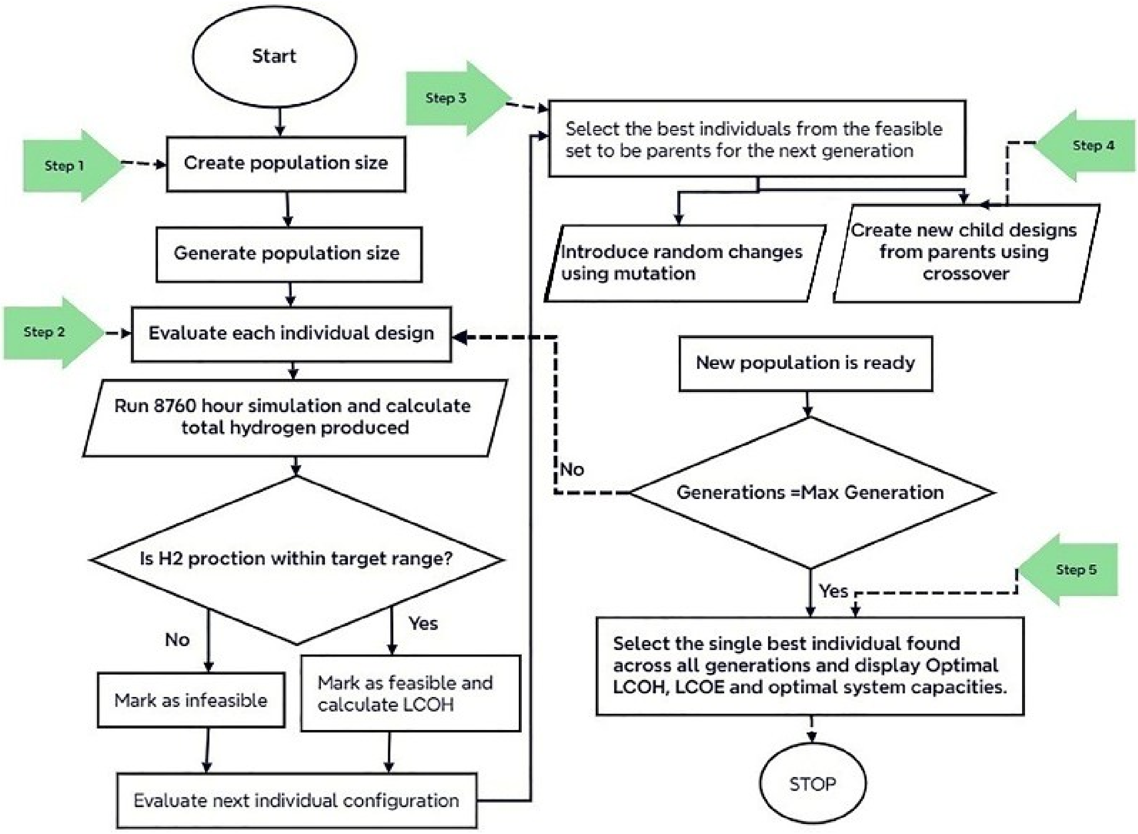

Figure 3. Genetic algorithm flowchart

Steps shown in **Figure 3** are further explained below.

- **Initialize Population**: Generate an initial set of random system designs, each with specific values for Wind (MW), Solar (MW), BESS (MWh), BESS (MW), and electrolyzer count, all within predefined bounds.
- **Simulation and Evaluation**: For each individual design, run a full 8760-hour simulation and evaluate nonlinear constraints to check if hydrogen production is within the target range (355,000 – 356,000 tons).
- **Selection**: Select the fittest individuals based on the lowest Levelized Cost of Hydrogen (LCOH); discard infeasible solutions that do not meet constraints.
- **Reproduction (Crossover and Mutation)**:
    - **Crossover**: Combine parameters from two parent designs to create new child designs.

  - **Mutation**: Introduce small, random changes to some children to maintain diversity and explore new configurations.
- **Repeat**: Iterate through simulation, evaluation, selection, and reproduction steps until convergence or stopping criteria are met.

Decision Variables and Constraints

The Genetic Algorithm seeks to find optimal values for the following five decisive variables:

- P_{Wind}: Wind Farm Capacity [MW];
- P_{Solar}: Solar PV Farm Capacity [MW];
- E_{Batt}: BESS Energy Capacity [MWh];
- P_{Batt}: BESS Power Capacity [MW];
- N_{Ely}: Number of Electrolyzer Units [Integer].

The vector of decision variables is defined by:

$$[x = P_{\text{wind}}, P_{\text{solar}}, E_{\text{Batt}}, P_{\text{batt}}, N_{\text{ely}}] \tag{28}$$

The following critical constraints govern the search for optimal solution:

- Production Target: The target ensures that the total annual hydrogen production falls within a specified range. For this analysis, the target is 356 000 tones/year.
- For each hour, the power supplied must equal the power consumed:

$$P_{\text{W,t}} + P_{\text{S,t}} + P_{\text{dis,t}} = P_{\text{Ely,t}} + P_{\text{char,t}} + P_{\text{curt,t}} \tag{29}$$

where are: $P_{\text{W,t}}$ and $P_{\text{S,t}}$ - the normalized power profiles for wind and solar; $P_{\text{dis,t}}$ - the power discharged from the BESS; $P_{\text{Ely,t}}$ - the power consumed by the electrolyzer bank; $P_{\text{char,t}}$ - the power used to charge the BESS, and $P_{\text{curt,t}}$ - any excess power that is wasted.

Electrolyzer Operational *Constraints*. Power supplied to the electrolyzer bank is a function of the number of active modules as given in eq. (30):

$$N_{\text{act.,t}} = \min\left(N_{\text{Ely,t}}, \left[\frac{P_{\text{W,t}} + P_{\text{S,t}} + P_{\text{dis,t}}}{P_{\text{unit,min}}}\right]\right) \tag{30}$$

The power consumed by the electrolyzer bank, $P_{\text{Ely,t}}$, must be within the operational range of the active modules.

$$N_{\text{act,t}} \times P_{\text{unit,min}} \leq P_{\text{Ely,t}} \leq N_{\text{active,t}} \times P_{\text{unit,rated}} \tag{31}$$

where are: $P_{\text{unit, min}}$ - the minimum power for one electrolyzer unit (7 MW); $P_{\text{unit,rated}}$ - the rated power for one electrolyzer unit (17.5 MW), and [·] is the floor function, ensuring only whole units can operate.

Battery State of Charge *operation*. The Battery Energy Storage System's State of Charge (SOC) is always maintained within its operational limits (30%≤$SOC(t)$≤90%).

Economic Model

In this study, a comprehensive economic analysis has been performed to evaluate the optimal LCOH. The approach used in this study is based on a standard Discounted Cash Flow (DCF) methodology, which accounts for the time value of money by discounting all future costs and production with respect to their present value. The total discounted cost over the project's lifetime is also referred to as the Net Present Cost (NPC) of the project. LCOH is defined in eq. (32) and eq. (33) [22]:

$$\mathrm{LCOH}[\frac{\mathrm{USD}}{\mathrm{kg}}] = \frac{\text{Net Present Cost}}{\text{Present Value (Lifetime } \mathrm{H_2} \text{ production)}} \tag{32}$$

This can be expanded to:

$$\mathrm{LCOH} = \frac{\mathrm{CAPEX_{total}} + \sum_{t=1}^{N} \frac{\text{annual costs}}{(1+i)^t}}{\sum_{t=1}^{N} \frac{\text{annual } \mathrm{H_2} \text{ produced}}{(1+i)^t}} \tag{33}$$

where are: $\mathrm{CAPEX_{total}}$ - the total initial capital expenditure at year 0; Annual Costs is the total recurring costs in year t, including fixed and variable operational & maintenance (O&M) costs for all components, as well as the cost of desalinated water; annual H_2 produced is the total mass of hydrogen produced in year t; i - the discount rate, representing the weighted average cost of capital (WACC); N - the economic lifetime of the project in years, and t - the specific year of the project lifetime.

SITE SELECTION

Site selection was informed by the strategic significance and potential of the available renewable energy resources and the availability of water. The area is located within the Tsau //Khaeb National Park in Lüderitz, Namibia. The study area shown in Figure 4 has also been selected for the first large- scale Hyphen green hydrogen project and is characterized by vast renewable energy resources, particularly high solar irradiance and consistent coastal wind.

Using the same site as Hyphen enables direct benchmarking with a real-world large-scale project, targeting about 355,000 tons of green hydrogen production per year using 7.5 GW of installed capacity with a 3 GW electrolyzer. In contrast to Hyphen's fixed sizing approach, this study aims to optimize renewable generation and electrolyzer capacities using a single-objective optimization strategy. The goal is to determine the most cost-effective system configuration with minimum LCOH, while ensuring an annual hydrogen production target is met or exceeded. By leveraging actual site data and conditions, the study will provide a practical and scalable insight into optimal system design for green hydrogen development in Lüderitz, Namibia.

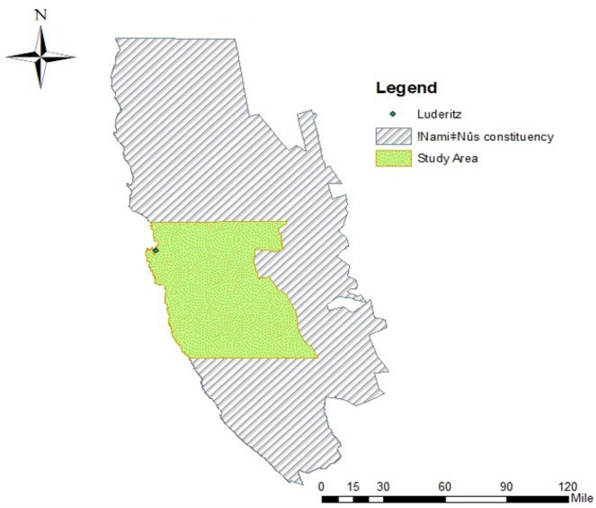

Figure 4. Study area at Lüderitz, Namibia.

Site Data

Figure 2, Figure 3 and Figure 4 show hourly ambient temperature, solar irradiation, and wind speed for a period of year, respectively. In Figure 5, temperature is observed to fluctuate between approximately 8 °C and 33 °C, with notable seasonal variation. Higher temperatures, ranging between 20 °C and 30 °C, are observed during summer months of January to March and October to December, while lower temperatures, often between 10 °C and 20 °C, dominate winter period of June to August. PV modules operate more efficiently, in winter seasons due to lower thermal losses Overall, the temperature range in the study area remains within operational limits for most PV technologies, making it suitable for year-round solar power generation.

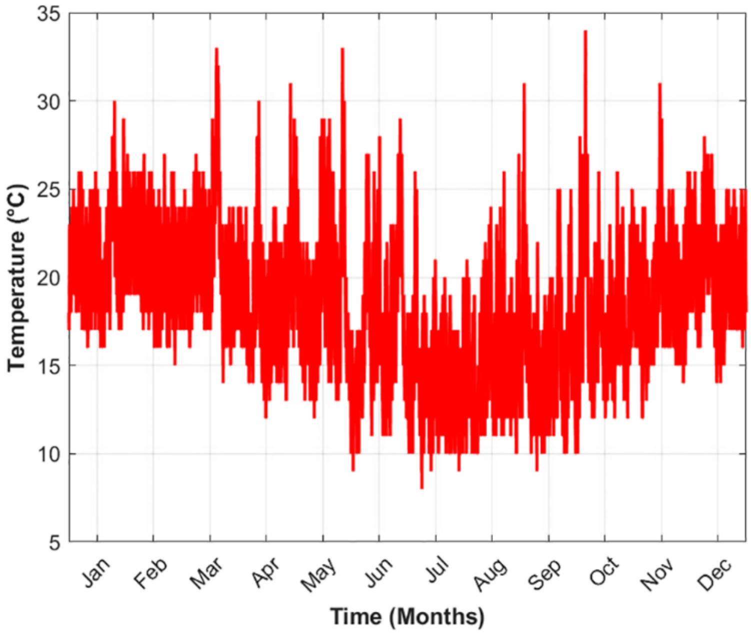

Figure 5. Lüderitz hourly ambient temperature data (2023)

In Figure 6 and Figure 7, it can be observed that both high solar irradiance and high wind speeds are experienced during the summer months. This prompts a need for an annual and robust optimization of hybrid RESs to meet the hydrogen set production target, with minimum storage capacity requirements.

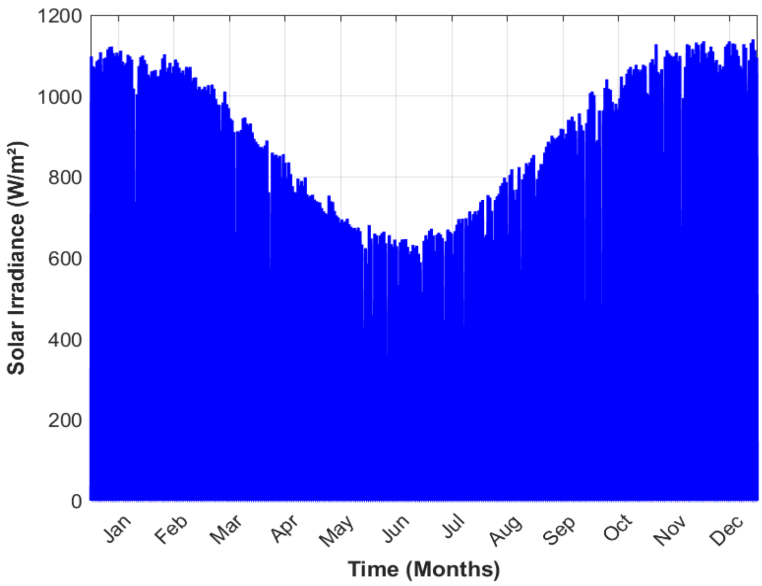

Figure 6. Lüderitz hourly solar irradiance data (2023)

Figure 6 highlights a clear seasonal trend, with daily irradiance values frequently exceeding 1000 W/m² during summer months, indicating strong solar potential. In contrast, winter period shows reduced irradiance levels, often ranging between 400 and 800 W/m², due to Earth's tilt angle from the sun during winter. Despite this variation, the overall irradiance remains consistently high throughout the year, affirming the study area as an excellent location for solar PV power generation.

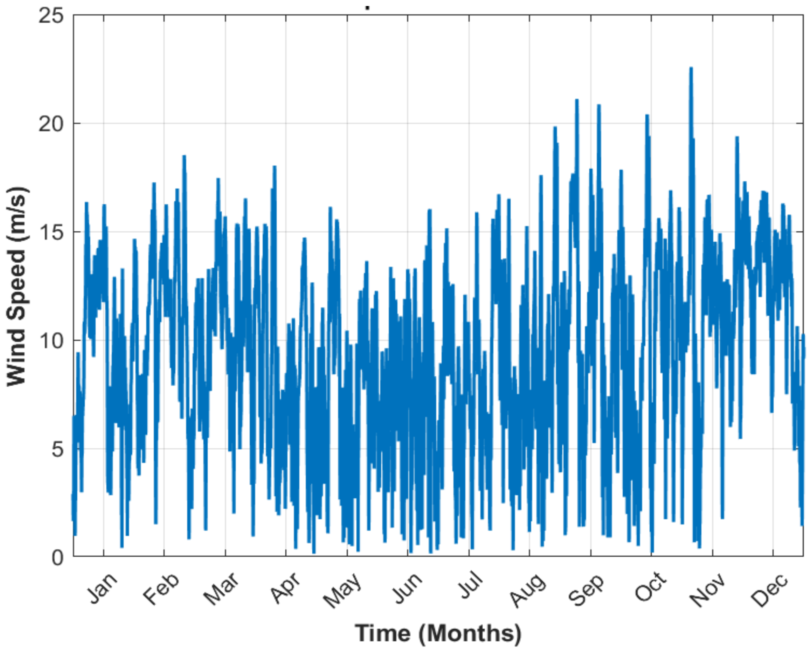

Figure 7. Lüderitz hourly wind speed data for 2023

Wind speed variation in Lüderitz shows frequent fluctuations throughout the year. The variation generally ranges between 2 and 15 m/s, with several peaks exceeding 20 m/s, indicating strong and consistent wind activity. Summer months exhibit slightly more frequent and higher wind speeds. This data demonstrates that Lüderitz experiences a robust and reliable wind resource throughout the year, making it a favorable location for wind energy generation.

OPTIMIZATION RESULTS

This section presents the results from techno-economic optimization model of the green hydrogen production facility. The analysis identifies the system configuration that achieves the minimum LCOH while satisfying the specified annual production target and operational constraints.

Optimal System Configuration and Economic Performance

GA successfully converged on a feasible solution that meets the annual production target of 355,000 - 356,000 tons of green hydrogen. The key economic performance indicators and the optimal system design are summarized in **Table 2**. The minimum LCOH achieved for the project was 2.5 USD/kg. This cost is underpinned by a Levelized Cost of Electricity (LCOE) of 0.0334USD/kWh for the renewable power system. The total lifetime cost of the project, represented by NPC, was obtained to be USD 8.72 billion. Results show that the optimal plant configuration is heavily reliant on wind power at 3,232 MW compared to 1,482 MW of solar PV. This 2:1 ratio shows that for the dataset used, wind provides a more consistent and economical source of energy for year-round hydrogen production.

Another key insight from system design is the relatively small battery system (500 MWh) in comparison to large renewable energy generation and electrolyzer capacities. This indicates that the most economical operational strategy is not to store enormous amounts of energy to run the plant continuously.

Table 2. Optimal system configuration and key performance indicators

Parameter	Optimal Value	Unit
Economic Performance		
Levelized Cost of Hydrogen (LCOH)	2.50	USD/kg
Levelized Cost of Electricity (LCOE)	33.39	USD/MWh
Net Present Cost (NPC)	8.72	USD billion
System Capacities		
Wind Farm Capacity	3232	MW
Solar PV Farm Capacity	1482	MW
BESS Energy Capacity	500	MWh
BESS Power Capacity	111	MW
Number of Electrolyzer Units	187	-
Total Electrolyzer Capacity	3272	MW

Annual Production Dynamics

Figure 8 illustrates the hourly rate of hydrogen synthesis, while Figure 9 illustrates cumulative production over the same period. Hourly hydrogen production profile reveals significant volatility throughout the year, highlighting the intermittent nature of RESs powering the system. Sharp and frequent peaks reach 62 645 kg/hour.

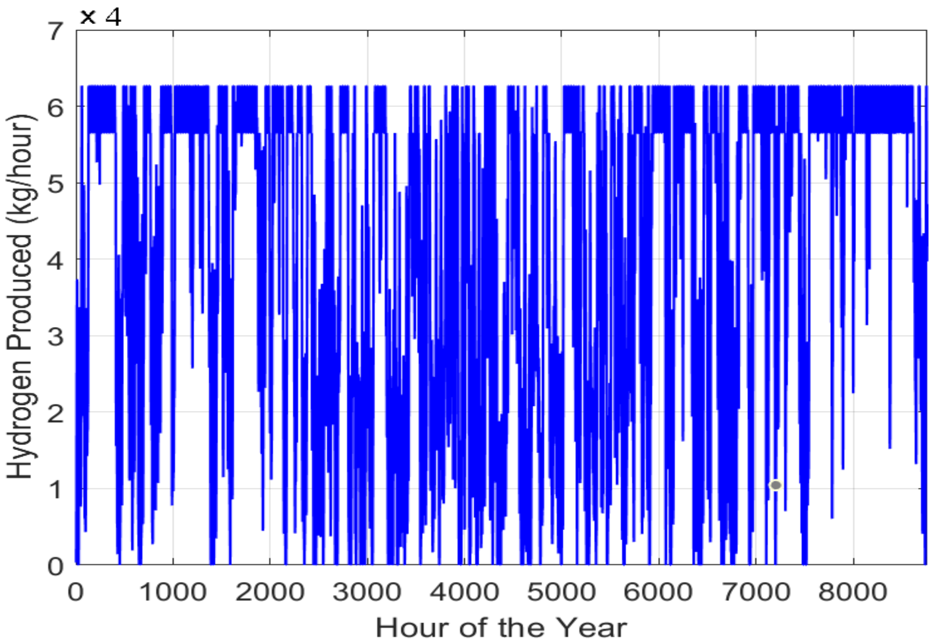

Figure 8. hourly hydrogen production rate for the optimal system configuration

These peaks correspond to daytime hours with clear skies and good wind speeds, particularly during the summer season. However, the graph also shows many instances of zero or near-zero production, especially during winter, and scattered throughout the entire year. These drops imply times of low resource availability due to nightfall, cloudy days, or calm wind conditions where renewable input is insufficient to sustain hydrogen generation, and BESS is discharged below minimum *SOC*.

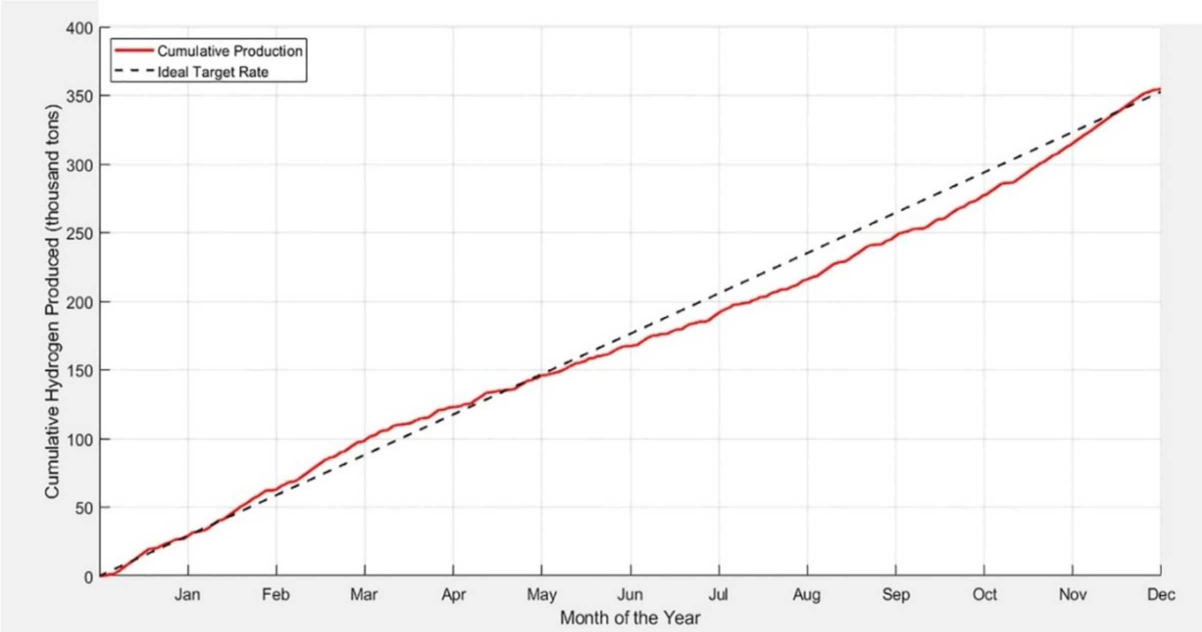

Figure 9. Optimal cumulative hydrogen production

Cumulative hydrogen production graph provides valuable insights into how seasonal variations affect system performance relative to annual targets. The actual production curve (red line) has noticeable fluctuations in slope throughout the year. During the first quarter of the year (January to March), the slope is relatively steep and above the ideal production target rate, indicating high production due to favorable weather conditions. In the mid-year period (April to September), the slope flattens, and production lags the ideal target line, suggesting reduced resource availability, which is also noticeable in the irradiance levels in **Figure 6** and low wind speeds shown in **Figure 7**. Toward the end of the year (October to December), the production rate increases thereafter, with the curve steepening and ultimately converging towards the ideal production target line, indicating a strong recovery during high-resource season. This trend demonstrates that while seasonal variability affects short-term production rates, high-production periods effectively compensate for earlier deficits, allowing the system to meet its cumulative annual hydrogen production target.

Electrolyzer Plant Efficiency

The operational efficiency of the electrolyzer bank is a critical factor in system's overall performance. **Figure 10** presents the distribution of plant's total loading state over the year, quantifying the number of hours the facility operates within various capacity brackets.

The analysis of the electrolyzer loading distribution reveals a highly effective and opportunistic operational strategy for the plant. The system operates in its peak loading state (80 – 100%) for a remarkable 5514 hours, which constitutes nearly 63% of the entire year. This indicates that the plant is primarily designed to maximize production by running at full capacity whenever renewable power is abundant.

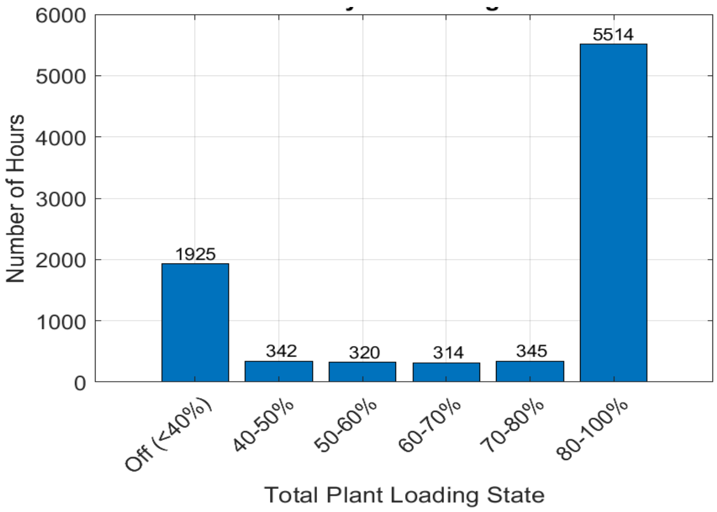

Figure 10. Annual electrolyzer loading distribution

The total operational uptime (loading >40%) is approximately 6,835 hours, corresponding to an annual availability of 78%. The distribution is highly polarized, with most hours spent at either peak load or off- load (1,925 hours). Relatively few hours are spent in the intermediate loading states (40 – 80%). This operational profile is a direct consequence of optimal system design. The large, combined capacity of the wind and solar farms allows the system to generate magnificent power, driving the electrolyzer bank to its maximum output. Conversely, the small battery system is not designed to sustain production through long periods of low renewable generation, leading to downtime. This confirms that optimization favored a strategy of lower capital expenditure by minimizing expensive battery storage over achieving constant, 24/7 plant utilization at rated capacity.

Sensitivity Analysis

Sensitivity analysis was performed by running the optimization for a range of electrolyser (150, 160, 170, 180, 190, and 200 units each rated at 17.5 MW). 17.5 MW was chosen because is the rating the commonly used PEM electrolyser (Elyser P- 300 by Siemens Energy. Results presented in **Figure 11**, reveal a critical trade-off between the capital expenditure on electrolyzers and the required investment in supporting renewable power infrastructure. **Figure 11** indicates that while adding more electrolyzers increases capital requirements (NPC), it does not necessarily lead to optimal cost of hydrogen production (LCOH).

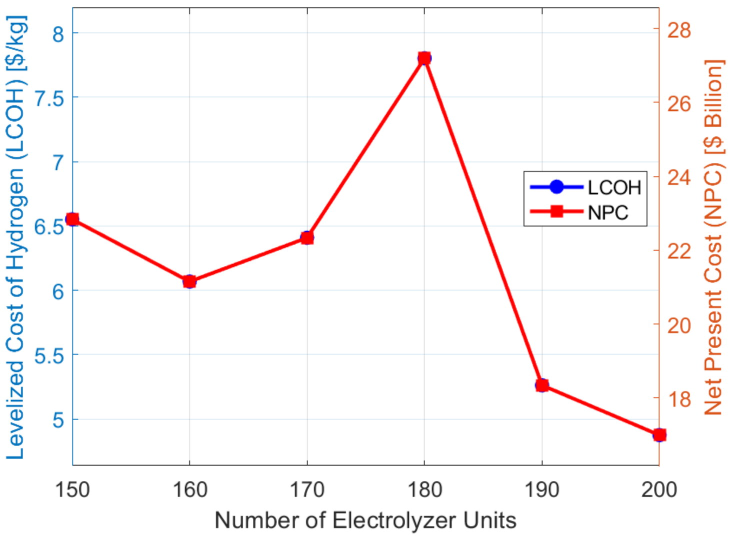

Figure 11. Economic performance vs electrolyser plant size.

The analysis demonstrates optimal number of electrolyser plant sizes that leads to optimal cost of hydrogen production is between 190-200 units, where both LCOH and NPC are minimized, whereas under-sizing (150 units) or suboptimal sizing (160 to 180 units) leads to poor economic outcomes.

Figure 12 illustrates the relationship between electrolyser plant size and system utilization. As more electrolyzer units are added, average utilization (capacity factor) decreases. This suggests that oversizing the plant relative to the available renewable energy supply reduces efficiency, since more capacity remains underutilized.

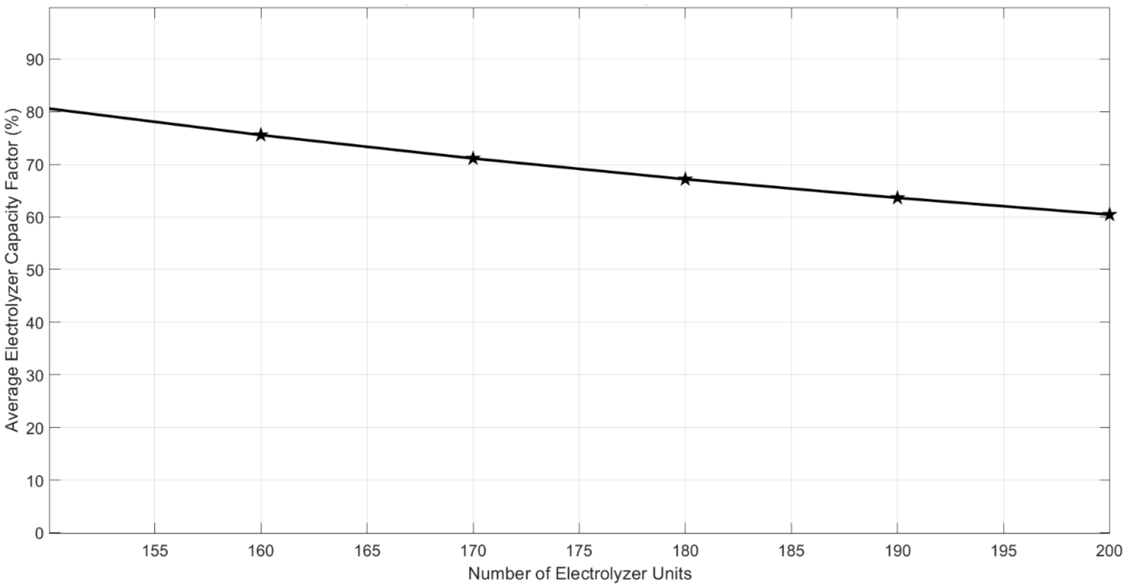

Figure 12. System utilization vs electrolyser plant size

CONCLUSION

This study developed an optimal techno-economic model to investigate the cost-effectiveness of the green hydrogen plant in Lüderitz, Namibia. The results of the optimized system gave an LCOH of 2.50 USD/kg compared to 7.5 USD/kg obtained from study on local hydrogen production analysis. This demonstrated the superior performance of the proposed algorithm. The primary conclusion of this work is that achieving cost-effective green hydrogen production from intermittent renewables is not contingent on achieving continuous operation, but rather on adopting an optimized, opportunistic production strategy.

Key finding from the optimal system design is the minimal reliance on energy storage. The Genetic Algorithm consistently favored over-building the renewable generation and electrolyzer capacities while minimizing the capital-intensive battery system. This allows the plant to capture and immediately convert low-cost electricity during periods of high wind and solar availability, while accepting downtime when resources are scarce. This approach was shown to be more economical than investing in the massive battery capacity required to force a constant, high utilization rate.

The value of this optimization is underscored when results were compared to publicly available data for the Hyphen Green Hydrogen project, a world benchmark in Namibia targeting a similar production scale. The Hyphen project is planned with approximately 7 GW of renewable capacity and 3 GW of electrolyzer capacity for an estimated investment of over USD 10 billion. In contrast, this study's optimized model achieves the same production target with a smaller renewable fleet (4.7 GW total) and a comparable electrolyzer capacity (3.3 GW), resulting in a significantly lower Net Present Cost of USD 8.72 billion. This suggests that a data-driven optimization, which tailors the wind-solar mix to the specific resource profile and minimizes reliance on storage, can unlock substantial capital savings compared to a more generic, un-optimized approach.

The findings have significant implications for the development of Namibia's green hydrogen economy, providing a robust framework for system sizing and investment planning. While this model provides a strong economic baseline, future work could expand upon this foundation by incorporating factors such as electricity market volatility, potential revenue from ancillary grid services, and the logistical costs of hydrogen storage and transport. Nonetheless, this study confirms that with proper system-level optimization, Namibia's abundant renewable resources can be leveraged to produce green hydrogen at a cost that is competitive on the global stage.

REFERENCES

1. A. Alzahrani, S. K. Ramu, G. Devarajan, I. Vairavasundaram, and S. Vairavasundaram, A Review on Hydrogen-Based Hybrid Microgrid System: Topologies for Hydrogen Energy Storage, Integration, and Energy Management with Solar and Wind Energy, *Energies 2022,* Vol. 15, No. 21, 2022, https://doi.org/10.3390/en15217979.
2. N. Kalaiselvan and T. Mathimani, Solar-driven green hydrogen generation for revolutionizing the future of zero-carbon energy, *Fuel*, Vol. 375, 2024, https://doi.org/10.1016/j.fuel.2024.132538.
3. IRENA, Renewable Power Generation Costs in 2020, in *International Renewable Energy Agency*, 2020, p. 160.
4. T. A. Deetjen, H. Martin, J. D. Rhodes, and M. E. Webber, Modeling the optimal mix and location of wind and solar with transmission and carbon pricing considerations, *Renew. Energy*, Vol. 120, 2018, https://doi.org/10.1016/j.renene.2017.12.059.
5. M. Zghaibeh, E. M. Barhoumi, P. C. Okonkwo, I. Ben Belgacem, W. H. Beitelmal, and I. B. Mansir, Analytical model for a techno-economic assessment of green hydrogen production in photovoltaic power station case study Salalah city-Oman, *Int. J. Hydrogen Energy*, Vol. 47, No. 31, 2022, https://doi.org/10.1016/j.ijhydene.2022.02.180.
6. M. R. Shaner, H. A. Atwater, N. S. Lewis, and E. W. McFarland, A comparative technoeconomic analysis of renewable hydrogen production using solar energy, *Energy Environ. Sci.*, Vol. 9, No. 7, 2016, https://doi.org/10.1039/c5ee02573g.
7. Green Hydrogen: Opportunities and Challenges in the Energy Transition – Global Renewables Congress.. https://renewablescongress.org/2025/02/green-hydrogen-opportunities-and-challenges-in-the-energy-transition/, [Accessed: Aug. 05, 2025].
8. D. Jovan and D. Gregor, Can Green Hydrogen Production Be Economically Viable under Current Market Conditions, *Energies*, Vol. 13, 2020, https://doi.org/10.3390/en13246599.
9. B. Akarsu and M. S. Genç, Optimization of electricity and hydrogen production with hybrid renewable energy systems, *Fuel*, Vol. 324, Part A, 124465, 2022, https://doi.org/10.1016/j.fuel.2022.124465.
10. S. S. Mohammad and S. J. Iqbal, Optimization and Power Management of Solar PV-based Integrated Energy System for Distributed Green Hydrogen Production, *Distributed Generation &Amp; Alternative Energy Journal*, Vol. 37, 2022, https://doi.org/10.13052/dgaej2156-3306.3741.
11. M. Zghaibeh *et al.*, Optimization of green hydrogen production in hydroelectric-photovoltaic grid connected power station, *Int. J. Hydrogen Energy*, Vol. 52, 2024, https://doi.org/10.1016/j.ijhydene.2023.06.020.
12. A. A. Alhussan, M. A. Saeed, A. Ibrahim, A. A. Abdelhamid, and M. M. Eid, Green hydrogen production ensemble forecasting based on hybrid dynamic optimization algorithm, *Front. Energy Res.*, Vol. 11, 1221006., 2023, https://doi.org/10.3389/fenrg.2023.1221006.

13. J. Park, S. Kang, S. Kim, H.-S. Cho, and S. Heo, Techno-economic analysis of solar powered green hydrogen system based on multi-objective optimization of economics and productivity, *Energy Convers. Manag.*, Vol. 299, No. 117823, 2024, https://doi.org/10.1016/j.enconman.2023.117823.
14. M. A. Albadr, S. Tiun, M. Ayob, and F. Al-Dhief, Genetic Algorithm Based on Natural Selection Theory for Optimization Problems, *Symmetry (Basel)*, Vol. 12, No. 11, 2020, https://doi.org/10.3390/sym12111758.
15. A. R. Olawale, S. Shodiya, and Y. H. Ngadda, Mathematical Modeling of Solar Photovoltaic Module to generate Maximum Power Using Matlab/Simulink, *Int. J. Appl. Technol. Res.*, Vol. 2, No. 1, 2021, https://doi.org/10.35313/ijatr.v2i1.46.
16. X. H. Nguyen and M. P. Nguyen, Mathematical modeling of photovoltaic cell/module/arrays with tags in Matlab/Simulink, *Environ. Syst. Res.*, Vol. 4, No. 1, 2015, https://doi.org/10.1186/s40068-015-0047-9.
17. M. T. Ahmed, T. Goncalves, A. Albino, M. R. Rashel, A. Veiga, and M. Tlemcani, Different parameters variation analysis of a PV cell, in *International Conference for Students on Applied Engineering, ICSAE 2016*, 2017, https://doi.org/10.1109/ICSAE.2016.7810183.
18. A. W. Manyonge, R. M. Ochieng, F. N. Onyango, and J. M. Shichikha, Mathematical modelling of wind turbine in a wind energy conversion system: Power coefficient analysis, *Appl. Math. Sci.*, Vol. 6, No. 89–92, 2012.
19. K. Thirugnanam, H. Saini, and P. Kumar, Mathematical Modeling of Li-Ion Battery for Charge / Discharge Rate and Capacity Fading Characteristics using Genetic Algorithm Approach, *2012 IEEE Transportation Electrification Conference and Expo,* Dearborn, MI, USA, 2012, https://doi.org/10.1109/ITEC.2012.6243431.
20. O. Demirci, S. Taskin, E. Schaltz, and B. Acar Demirci, Review of battery state estimation methods for electric vehicles - Part I: SOC estimation, *J. Energy Storage*, Vol. 87, 111435, 2024, https://doi.org/10.1016/j.est.2024.111435.
21. Electric load for electrolyzer - MATLAB - MathWorks Deutschland. https://de.mathworks.com/help/sps/ref/electrolyzer.html?s_eid=PSM_15028#mw_b2901d5d-22ff-4178-92df-ca84973e63fd, [Accessed: Aug. 12, 2024].
22. O. Tang, J. Rehme, and P. Cerin, Levelized cost of hydrogen for refueling stations with solar PV and wind in Sweden: On-grid or off-grid?, *Energy*, Vol. 241, 122906, 2022, https://doi.org/10.1016/j.energy.2021.122906.

Paper submitted: 17.09.2025
Paper revised: 09.01.2026
Paper accepted: 05.02.2026